arXiv:cond-mat/0510382v1 [cond-mat.mes-hall] 14 Oct 2005

Scaling Law in Carbon Nanotube Electromechanical Devices

R. Lefèvre[1], M. F. Goffman[1*], V. Derycke[1],

C.Miko[2], L. Forró[2], J. P. Bourgoin[1] and P. Hesto[3]

[1]*Laboratoire d'Electronique Moléculaire, CEA-DSM SPEC,*

CEA Saclay, 91191 Gif-sur-Yvette, France

[2]*EPFL, CH-1015, Lausanne, Switzerland*

[3]*Université Paris 11, Institut d'Electronique Fondamentale,*

*CNRS, UMR 8622, F-91405 Orsay, France**

Abstract

We report a method for probing electromechanical properties of multiwalled carbon nanotubes(CNTs). This method is based on AFM measurements on a doubly clamped suspended CNT electrostatically deflected by a gate electrode. We measure the maximum deflection as a function of the applied gate voltage. Data from different CNTs scale into an universal curve within the experimental accuracy, in agreement with a continuum model prediction. This method and the general validity of the scaling law constitute a very useful tool for designing actuators and in general conducting nanowire-based NEMS.

PACS numbers: 62.25.+g, 85.85.+j, 46.70.Hg

*Corresponding author email address: goffman@cea.fr

Carbon nanotubes (CNTs) are promising candidates for designing and developing nano-electromechanical systems (NEMS) because they combine excellent electronic and mechanical properties. High conductivity of CNTs allows for designing simple sensing and actuation systems based on the direct electrostatic coupling with metallic gates. Their exceptional stiffness, low mass and dimensions ensure operating frequencies in the GHz range making them suitable for a number of applications[1]. Some prototypes of CNT-based NEMS such as memory devices[2], nanotweezers[3], high frequency oscillators[4] and actuators[5] have already been demonstrated. Theoretical studies of CNT-based switches have been recently published[6][7][8]. Particularly interesting are molecular dynamics simulations of Dequesnes and coworkers[6] which have made evident the validity of continuum models (beam theory) in describing CNT deformation when its length/diameter ratio is larger than 10. This is a very important point because it simplifies the description of CNT mechanical deflection avoiding expensive and time consuming atomistic simulations. However, designing CNT-based NEMS requires a very precise knowledge of the static deflection under actuation. Since in most of the CNT-based NEMS actuation is electrostatic the relevant parameters are: the geometry of the CNT (inner and outer diameter, length), its Young's modulus Y, and the geometry of the device which conditions the CNT- gate(s) electrostatic coupling and thus the actuation efficiency. The interplay between the different geometrical parameters indeed makes theoretical prediction tools indispensable to properly scale any practical device based on suspended CNTs. Comparison with experiments is equally important both to evaluate the validity of the predictions and precisely measure Y, since it determines most of the static and dynamic properties of CNTs.

In this letter, we report an on-chip test method for measuring the deflection of suspended and electrostatically actuated CNTs. We develop a theoretical framework for the modelisation of the electromechanical behavior of CNTs based on continuum models and validate it experimentally using that test method. Furthermore, we determine the CNT-Young's modulus[9][10] [11] [12][13] very precisely. The heart of the system is a doubly clamped suspended CNT three-terminal device (see Fig. 1) deflected by an electrostatic force induced by a back gate. In this geometry, Van der Waals forces[6] can be neglected. The CNT deflection only depends on its physical properties and on the electrostatic environment given by the connecting and gate electrodes, thus allowing a quantitative comparison with calculations. We measured the maximum deflection u_{MAX} ($u_{MAX} \equiv H - \mathrm{y}(L/2)$) see Fig. 1a) of

a suspended multiwalled CNT as a function of the applied gate voltage V_G. We show that data from different CNTs (with different diameters D and lengths L) scale into an universal curve within experimental uncertainties. This scaling law that we derived from continuum beam theory when $u_{MAX} \ll D$, can be extended to the $u_{MAX} \geq D$ range, where the induced stress T due to elongation of the CNT becomes important. Furthermore it is also valid in the general case where there is an electrostatic force profile applied along the CNT. The set of consistent data allows us to accurately determine $Y = 0.41 \pm 0.05$ TPa. Our method and the general validity of the scaling law constitute a very important outcome for designing conducting nanowire-based NEMS.

A schematic diagram and a typical SEM picture of a CNT-based device is presented in Fig. 1. A multiwalled CNT of diameter D is clamped by two metallic pads and suspended over a length L on top of a highly doped silicon substrate that acts as a gate. The distance between the CNT and the gate is fixed by the sacrificial silicon dioxide layer thickness H (230 nm in the present case). The multiwalled CNTs used were synthesized by arc-discharge evaporation and carefully purified to remove amorphous carbon and graphitic nanoparticles[14]. The sample were fabricated as follows: some droplets of a sonicated suspension of CNTs in dichloroethane (50 μ g/ ml) are deposited on an oxidized Si wafer, and blown dry after one minute under nitrogen flow. Atomic force microscopy[15] is used to image, select, and locate CNTs with respect to pre-patterned alignment marks. Selected CNTs are then connected with two electrodes designed by electron beam lithography, and deposited by thermal evaporation of gold (70 nm) with a chromium adhesion layer (0.5 nm). These metallic electrodes are used both as conducting electrodes and anchor pads. The sample is dipped in BHF to remove all the SiO_2 underneath CNTs, rinsed in DI water and ethanol and dried on a hot plate at 50°C.

The sample is mounted in a commercial AFM equipped with a conducting tip. CNTs and AFM tip are grounded, in order to avoid any electrostatic interaction between them[16]. To measure the deflection of the CNT when a voltage V_G is applied to the back-gate electrode, the AFM is used in the tapping mode. The experimental setup is depicted in the insert of Fig. 2. The AFM tip is placed and immobilized[17] at the center of the CNT. The feedback voltage applied to the piezoelectric element V_{piezo}, that controls the vertical position of the tip, is monitored as a function of V_G. Fig. 2 shows a typical result for a suspended CNT, 600 nm long and 10 nm in diameter (device #1). As $|V_G|$ increases, the CNT deflects

downwards, the AFM tip has more room to oscillate and the oscillation amplitude increases. To keep constant the oscillation amplitude of the tip, a positive V_{piezo} is applied by the AFM electronics. The measured V_{piezo}, proportional to the deflection of the CNT, is found to vary as V_G^2. This is expected for a CNT that follows the Hooke's law, because the applied force is proportional to V_G^2 (see Eq.3 below). The AFM tip position is also influenced by the electrostatic attraction to the substrate. Indeed, when the tip is placed on the sacrificial silicon dioxide layer at the same CNT-gate distance (position 2 in Fig. 2), increasing $|V_G|$ increases the attractive electrostatic force between the tip and the substrate, the oscillation amplitude decreases and a negative V_{piezo} is applied by the feedback loop. The genuine CNT deflection is obtained by subtracting from the curve measured at position 1 the one measured at position 2 previously divided by the relative permittivity of the silicon dioxide (dotted line in Fig.2)[18].

We repeated the experiment on four devices with different L and D parameters[19]. Using the calibration of the piezoelectric element[20] (243.8 nm/ V) the deflection of the CNT, u_{MAX}, can be obtained as a function of the applied V_G. Fig. 3a shows results for three different devices: #1 ($L = 600$ nm, $D = 10$ nm), #2 ($L = 770$ nm, $D = 13.5$ nm) and #3 ($L = 480$ nm, $D = 10$ nm). The parabolic behavior is made evident in this Log-Log scale representation (the dotted line is a guide to the eye that has V_G^2 dependence).

The strong dependence of $u_{MAX}(V_G)$ on different CNT parameters (L and D) can be understood using a continuum beam equation[21] for describing the deflection of the CNT (denoted by y(x)) when an electrostatic force per unit length F_{elec} is applied. In reduced units ($y = \mathrm{y}/D$ and $x = \mathrm{x}/L$) this equation reads

$$\frac{d^4y}{dx^4} - \frac{TL^2}{YI}\frac{d^2y}{dx^2} = \frac{L^4}{YID}F_{elec}(y, D, V_G) \tag{1}$$

Here Y is the Young's modulus (typically of the order of 1 T Pa[9]-[13]) and I the moment of inertia of the CNT approximated[22] by $I = \pi D^4/64$. T is the stress force induced by elongation of the CNT when the electrostatic force $F_{elec}(y, D, V_G)$ is applied. T can be calculated by,

$$T = \frac{\pi D^4 Y}{8L^2}\int_0^1 \left(\frac{dy}{dx}\right)^2 dx \tag{2}$$

To solve Eq.1 , we have to assume that the stress force T has a constant value, which is ob-

tained later from the self-consistent condition (Eq.2). The electrostatic force $F_{elec}(y, D, V_G)$ can be modeled by considering the electrostatic energy $E_{elec} = \frac{1}{2}C(y, D)V_G^2$ and the principle of virtual work[23], $C(y, D)$ being the capacitance per unit length of a CNT over a metallic plane. This force has the form:

$$F_{elec}(y, D, V_G) = \frac{2\pi\varepsilon_0 V_G^2}{D} g(2y) \tag{3}$$

Where ε_0 is the permittivity of vacuum and $g(t) = \left[\sqrt{t(t+2)}\ln^2\left(1 + t + \sqrt{t(t+2)}\right)\right]^{-1}$. This function can be well approximated in the range of practical interest[24] by $g(t) = A\,t^{-\beta}$ with $A = 0.270$ and $\beta = 1.456$. Since in our case $H \gg u_{MAX}$, considering the electrostatic force (at a given V_G) as a constant is a good approximation. This is strictly true for an infinite geometry. Indeed, contacting electrodes modify the electrostatic force near the CNT-metal interface due to screening and the AFM tip (in spite of being at the same potential as the CNT) modifies the electrostatic force near its position. We calculated the electrostatic force profile that builds up by 3D numerical simulations (FEMLAB) of our structures. It turns out that the deflection of the CNT produced by the electrostatic force profile is equivalent to the one generated by a constant force $F_{elec}(H, D, V_G)$ times a correcting factor. This factor C_{FP}, is: 1.26 for device #1, 1.28 for #2, 1.45 for device #3 and 1.21 for device #4 (L = 730 nm, $D = 15$ nm) [25].

It is interesting to note that the second term in Eq.1 is negligible[26] at low V_G, where $u_{MAX} \ll D$. In this limit the maximum deflection is well approximated by

$$\frac{u_{MAX}}{D} = K\left(\frac{V_G L^2}{D^{3-\beta/2}}\right)^2 \quad , \quad K = \frac{C_{FP} A \varepsilon_0 (2H)^{-\beta}}{3Y} \tag{4}$$

Fig. 3 depicts the results on the four devices rescaled using Eq.4. The curves indeed collapse onto a single curve within the experimental accuracy in determining L and D. This finding implies that Y is nearly the same for all the devices investigated, in agreement with theoretical predictions[27]. Furthermore, it allows a quantitative determination of the Young's modulus as shown in the insert of Fig. 3b, where the points represents Y calculated from the data using Eq.4 for the four devices investigated. The average Y value obtained from these experiments is 0.41 ± 0.05 T Pa. This value is smaller than expected compared to previous measurements, although it is statistically indistinguishable from the one obtain by J. P. Salvetat *et al.* [12] on the same source of CNTs. One possible explanation

might be defects induced either by the purification treatment or by the lithographic steps. Experiments are underway to examine these issues.

In order to explore the validity of the scaling law predicted and experimentally observed at low deflections, we solved Eq.1 on a larger V_G range. Fig. 4a shows the calculated maximum deflection of the CNT (u_{MAX}) as a function of V_G for the structure depicted in Fig. 1a. Different curves correspond to different D, L parameters (experimentally accessible) for a fixed H value. Since H is still much greater than u_{MAX}, considering the electrostatic force along the CNT as a constant remains a good approximation. Notice the large variation of $u_{MAX}(V_G)$ when L or D varies. This simply reflects the strong dependence on geometrical parameters. Now, if the curves depicted in Fig. 4a are rescaled according to Eq.4 a collapse onto a single curve is made evident (see Fig. 4b). This scaling law, expected at low V_G as shown above, proves to be valid in the whole range investigated. This striking result observed for a constant force per unit length can be generalized to the case of multiple gates as long as the functional form of the force profile along the CNT is the same for devices with different L and D[25].

In conclusion, we have presented an accurate method for probing the electromechanical properties of suspended nanotubes and measuring the Young's modulus using a conducting AFM on a simple test bench structure. In this method the maximum deflection u_{MAX} of the CNT is measured as a function of an electrostatic force controlled by V_G. It was shown that $u_{MAX}(V_G)$ can be rescaled into an universal curve that only depends on the geometrical parameters of the structure (L, D and H) and on Y. This scaling law, together with our on-chip method constitutes a very useful tool for designing actuators and in general CNT-based NEMS where a precise knowledge of static deflection is required. We note that the principle of the method used here can be extended to other geometries like that of suspended cantilever or multiple gate structures.

We thank D. Dulić for critical reading of the manuscript. The research has been supported by ACI "nanosciences et nanotechnologies" programs (CNRS) and the Swiss National Science Foundation and its NCCR "Nanoscale Science".

---

[1] A.N. Cleland, *Foundations of Nanomechanics,* Springer-Verlag, Berlin (2003).

[2] T. Ruekes *et al.*, Science **289**, 94 (2000).

[3] P. Kim and C. M. Lieber, Science **286**, 2148 (1999).

[4] V Sazonova *et al.*, Nature **431**, 284 (2004).

[5] R. H. Baughman *et al.*, Science **284**, 1340 (1999).

[6] M. Dequesnes, S. V. Rotkin and N. R. Aluru, Nanotech. **13**, 120 (2002).

[7] J. M. Kinaret, T. Nord and S. Viefers, Appl. Phys. Lett. **82**, 1287 (2003).

[8] S. Sapmaz *et al.*, Phys. Rev. B **67**, 235414 (2003).

[9] M. M. J. Treacy, T. W. Ebbesen and J. M. Gibson, Nature **381**, 678 (1996); B. Babiæ, *et al.*, Nanolett. **3**, 1577 (2003).

[10] P. Poncharal *et al.*, Science **283**, 1513 (1999).

[11] E. W. Wong, P. E. Sheehan and C. M. Lieber, Science **277**, 1971 (1997).

[12] J. P. Salvetat *et al.*, Appl. Phys. A **69**, 255 (1999).

[13] B.G. Demcsyk, *et al.*, Mat. Sci. Eng. A**334**, 173, (2002).

[14] J. M. Bonard, *et al.*, Adv. Mater. **9**, 827 (1997).

[15] No scanning electron microscopy was used to avoid any damage on CNTs, see for more details, F. Beuneu *et al.,* Phys. Rev. B **59**, 5945 (1999).

[16] In general a static charge can be present even when the tip and the CNT are at the same ground potential. This charges, related to the difference between work functions of the materials involved, are equilibrated each time the tip and the CNT enter into contact during the oscillation of the tip.

[17] Scanning in the plane is switched off. The system is stable enough to ensure a reproducible result.

[18] We proved this fact by performing an experiment on the same CNT with two different cantilevers with different sensitivity to the tip-gate attraction.

[19] L was estimated from SEM images of the devices and D from AFM images before CNT suspension.

[20] This value takes into account the electronic gain of the AFM controller.

[21] L. D. Landau and E. M. Lifshitz, *Theory of Elasticity*, Pergamon Press, Oxford (1986).

[22] In general I is estimated with $\pi\left(D^4 - D_i^4\right)/64$, where D_i is the inner diameter of the CNT. However the value of K (see text) is insensitive to D_i , because when $D_i/D = 1/3$, which is an extreme case, K differs only by 1% as compared with $D_i = 0$.

[23] R. P. Feynman, R. B. Leighton and M. Sands, *The Feynman Lectures on Physics*, Vol.III,

Addison Wesley (1977).

[24] In our case this region was taken in the $10 < y < 50$ range. The slight dependence of β on y does not change any conclusion of our work.

[25] M. F. Goffman *et al.*, to be published.

[26] See Ref.[20] p.79.

[27] Jian Ping Lu, Phys. Rev. Lett. **79**, 1297 (1997).

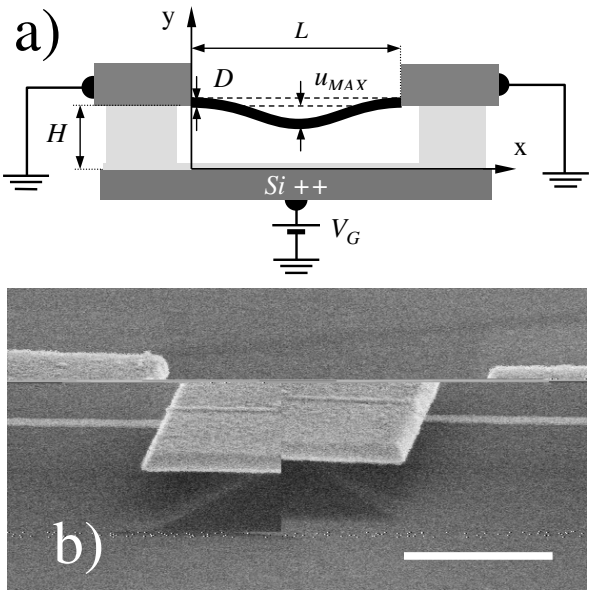


FIG. 1: a) Schematic picture of a nanoelectromechanical doubly clamped suspended CNT three terminal device. The distance between the CNT and the back gate electrode is labeled as H. L denotes suspension length and D the external diameter of the CNT. The deviation from the straight line is denoted by y(x). b) SEM image of a typical device used in AFM experiments (scale bar: 500 nm). The CNT is connected with two metallic electrodes, used both as conducting electrodes and anchor pads. The heavily n doped Si substrate (10^{19} cm^{-3}) act as a back-gate.

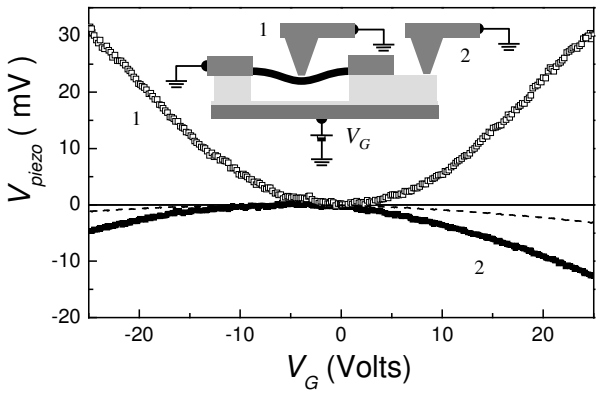


FIG. 2: Feedback voltage applied to the piezoelectric element V_{piezo} as a function of the gate voltage V_G at two different positions on device #1 ($L = 600$ nm, $D = 10$ nm): 1 at the middle of the CNT ; 2 on the sacrificial oxide of the silicon substrate (see insert). In the first case, increasing $|V_G|$ produces the deformation of the CNT, the cantilever tip has more room to oscillate and the oscillation amplitude increases. To maintain constant the oscillation amplitude of the tip (tapping mode), a positive V_{piezo} is applied by the feedback loop. Conversely, in the second case, increasing $|V_G|$ increases the attractive electrostatic force between the tip and the substrate, the oscillation amplitude decreases and a negative V_{piezo} is applied by the feedback loop. The actual CNT deflection is obtained by subtracting from the curve measured at position 1 the one measured at position 2 previously divided by the relative permittivity of the silicon dioxide (dotted line).

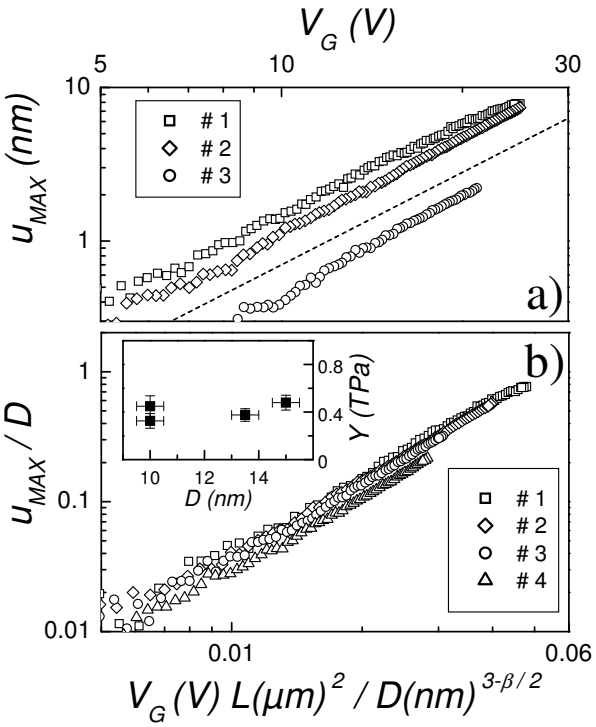


FIG. 3: a) Maximum deflection u_{MAX} as a function of V_G for devices #1 ($L = 600$ nm, $D = 10$ nm), #2 ($L = 770$ nm, $D = 13.5$ nm) and #3 ($L = 480$ nm, $D = 10$ nm). Dash line: guide to the eye that has V_G^2 dependence. b) u_{MAX} as a function of V_G rescaled using Eq.4 (see text) for four different devices: #1,#2,#3 and #4 ($L = 730$ nm, $D = 15$ nm). Insert: Calculated Young's modulus obtained from the scaling constant K (Eq.4) for the four devices. Error bars are estimated from the uncertainty on L and D.

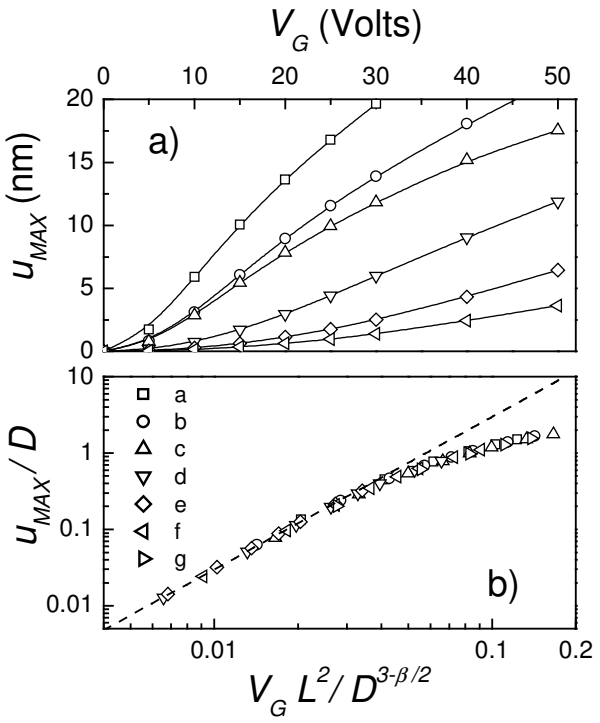


FIG. 4: a) Calculated maximum deflection u_{MAX} as a function of V_G for different L, D parameters: a ($L = 1200$ nm, $D = 13$ nm), b ($L = 1000$ nm, $D = 13$ nm), c ($L = 800$ nm, $D = 10$ nm), d ($L = 800$ nm, $D = 15$ nm), e ($L = 800$ nm, $D = 20$ nm), f ($L = 500$ nm, $D = 13$ nm), g ($L = 800$ nm, $D = 8$ nm). b) Same results rescaled according to Eq.4 (see text). Dash line: Analytical result obtained for induced stress $T = 0$.